Third International Conference on Energy, Materials, Applied Energetics and Pollution
ICEMAEP2016, October 30-31, 2016, Constantine,Algeria
M.KADJA, A.ZAATRI, Z.NEMOUCHI, R.BESSAIH, S.BENISSAAD and K. TALBI (Eds.)

FLOW DYNAMICS OF AN IMPINGING PLANE JET GENERATING SLOT TONES

Nabil KHAROUA[1], Lyes KHEZZAR[2], Mohamed ALSHEHHI[3]

[1]Mechanical Engineering Department, Petroleum Institute, Abu Dhabi, UAE, nkharoua@pi.ac.ae
[2] Mechanical Engineering Department, Petroleum Institute, Abu Dhabi, UAE, lkhezzar@pi.ac.ae
[3] Mechanical Engineering Department, Petroleum Institute, Abu Dhabi, UAE, malshehhi@pi.ac.ae

ABSTRACT

A plane jet, impinging on a slotted surface, was studied using Large Eddy Simulation LES. The slotted surface was placed a distance equal to four times the jet width. The Reynolds number, based on the jet width and the mean inlet velocity was equal to 5435. The interaction of the jet with the slot generates self-sustained noise.

The dynamic field of the turbulent flow was explored to investigate the high and low pressure zones directly related to the behavior of the coherent structures generated within the two plane free-shear layers developing on either side of the jet. These coherent structures might travel in parallel pairs causing a throttling phenomenon to occur when they interact with the slot. The slot toones are strongly related to such phenomena.

Key Words: *Impinging jet, Slot tone, Vortices, Fluctuating pressure, Large Eddy Simulation*.

NOMENCLATURE

Symbols :		**Indices / Exponents :**	
H	Jet and slot width, m	0	At inlet
w	Streamwise velocity, m/s	rms	Root mean square
x,y,z	Coordinates, m		

1. INTRODUCTION

Turbulent plane jets impinging on slotted surfaces generate noise in the form of slot tones depending on the Reynolds number and the jet exit-to-impingement surface distance. The tones appear when the turbulence and sound characteristic frequencies are in phase corresponding to an establishment of a feedback loop [1]. The understanding and control of the airborne sound is relevant to industrial applications of air conditioning, ventilation, solid-fuel rocket motors and whistling kettles [2, 3].

Blake and Powel [4] presented some important aspects of the slot tone in their review on different applications. Studies focusing on the slot tone appeared in the 1990s, e.g., [5]. A series of experimental studies were conducted within the research group of University of La Rochelle on the slot tones [3, 6]. Assoum [3] presented more details about the dynamic field, within the space separating the jet exit and the obstacle, and its correlation with the acoustic signals. The results were summarized in spatio-temporal cross-correlation maps.

Recently, the rapid advance of computational tools motivated the research community to develop different numerical approaches to tackle aeroacoustics problems. Reviews such as those of Tam [7] or Bodony and Lele [8] addressed the classical case of free jet to establish the best practice guidelines for the aeroacoustics simulation. Two main approaches were developed including the direct method and the hybrid method. The direct method is intended to resolve the coupled dynamic and acoustic fields explicitly while the hybrid method separates the two fields.

Several interesting numerical studies do exist in the literature on edge tones [9], hole tones [2, 10-11] and slit tones [12-13]. Numerical simulations of the slot tones seem to be inexistent in the literature. Since the hole tone is similar to the slot tone, insightful findings from the related literature will be described herein. Matsuura et al. [2] simulated the hole tone using a direct method. They observed a previously unknown feedback loop which occurs inside the jet itself. Matsuura et al. [10] elucidated the throttling mechanism for the same configuration of hole tone. The throttling mechanism occurs due to the variation of pressure at the impingement hole under the effect of the passing vortices. The previous studies allowed Matsuura et al. [11] to propose the suppression of the hole tones using an obstacle placed within the wall jet at a certain distance from the hole edge depending on the flow characteristics.

Based on the literature of free and impinging jet noise, it can be concluded that acoustics increases the complexity of jet simulation due to different spatial and temporal scales compared with those of turbulence in addition to the special care needed for the boundary conditions. LES and DNS approaches are highly recommended for accuracy purposes especially for the near-field while the analogy method is necessary if the far-field noise is to be predicted.

In the present study, LES is used to simulate the plane turbulent jet impacting a slotted plate at a Reynolds equal to 5435, based on the jet-exit velocity and width. The distance separating the jet exit and the slotted surface is four times the jet-exit width. The present LES simulation is intended to complement the experimental study of Assoum [3] by exploring further the complex dynamic field resulting from the interaction of the coherent structures with the slot. The focus will be on the pressure field.

2. NUMERICAL APPROACH

2.1. Mathematical and numerical modeling assumptions

The Large Eddy Simulation approach, as implemented in ANSYS FLUENT 16.2 [14], is used in this study and is based on the Wall-Adapting Local Eddy-Viscosity (WALE) model under Favre-averaging of the Navier-Stokes equations.

2.2. Computational mesh

The Cross-section of the geometry is presented in Figure 1. The slotted plate is placed at a distance equal to four times the jet-exit width (inlet of the computational domain). A multi-block structured hexahedral grid was generated in most of the computational domain (Figure 1). The computational domain was divided into 3.9 and 19 million cells representing a coarse and fine mesh, respectively. The grids were assessed from an LES viewpoint which is to generate an optimal mesh size within the Taylor microscale range allowing the capture of the most energetic turbulent structures [15-17]. The grid was refined in the two free jet regions upstream and downstream of the impingement plate, the impingement region, and the two wall jets. Based on a RANS (Reynolds Averaged Navier-Stokes) simulation, the ratio of the mesh size to the Kolmogorov scale was less than 14 and 10 for the coarse and fine grids, respectively which is compatible with the value of 12 recommended by the literature [18]. In addition, the computational cells are smaller than twice the Taylor microscale in the whole domain apart from the wall-adjacent nodes. The non-dimensional distance from the curved wall (y+) was smaller than 1 in the wall jet region for both grids.

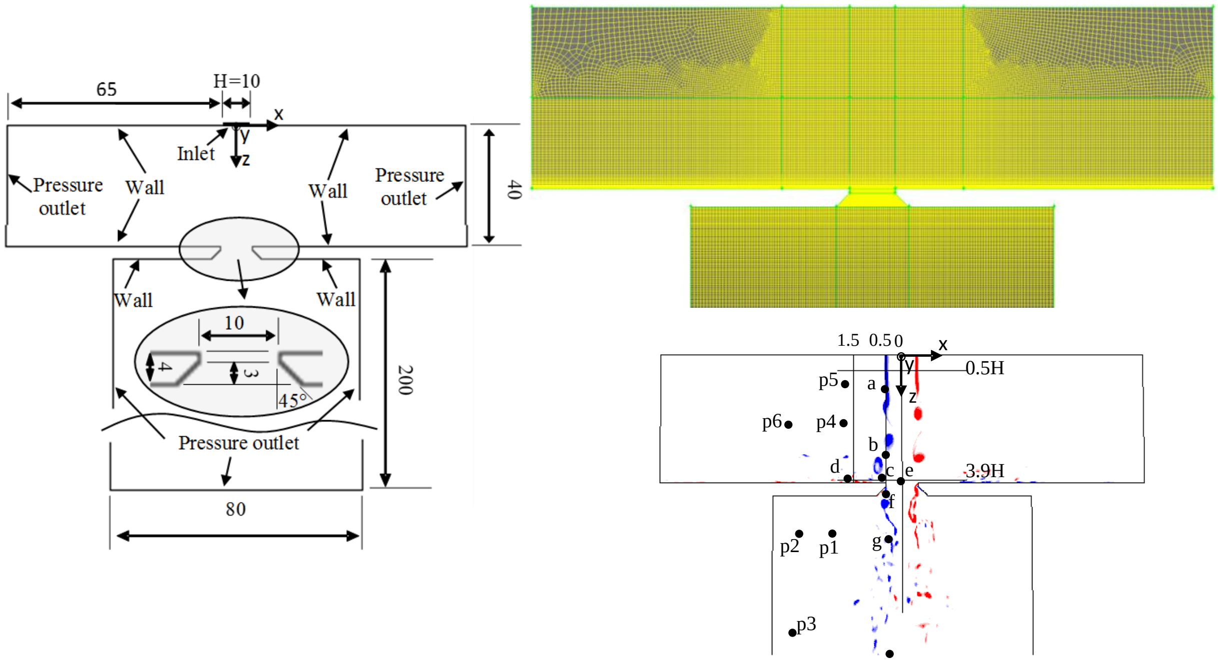

FIGURE 1. Geometry, mesh and boundary conditions

2.3. Boundary conditions

At the inlet of the computational domain, a velocity profile was imposed. A turbulence intensity, equal to 2%, was prescribed based on the experimental work of [3]. The spectral synthesizer technique [14] was used for the generation of fluctuating velocity components. Non slip boundary condition was imposed at the walls. An atmospheric pressure was imposed at the remaining boundaries of the computational domain in conjunction with the Non-Reflecting Boundary Condition option [14] to avoid the reflection of spurious pressure waves. A periodic boundary condition was applied at the opposite surfaces in the y direction to reduce the computational domain and optimize the computational grid based on Versteeg and Malalasekra [19] recommendation of at least twice the turbulent length scale of the problem between the two surfaces.

2.4. Numerical tools and simulation strategy.

The simulations consisted of four steps. In the first step, a steady flow field was obtained using the k-ω SST model to generate a good first guess for the transient LES simulations. Secondly, transient LES simulations were run with time step equal to 10^{-5} s until a statistical convergence was reached after 10 cycles based on a characteristic frequency of 100Hz extracted from the present case frequencies. For the third step, another transient simulation was conducted while imposing the Non-Reflecting Boundary Condition with a smaller time step (2.5×10^{-6} s) during 5 cycles. The last step was required to collect the flow statistics during more than 10 cycles.

The simulations were run using 48 and 96 parallel processors for the coarse and fine grids, respectively, during 3000 hours of CPU time.

3. RESULTS AND DISCUSSION

In the present work, the points and lines shown in Figure 1 were used to collect the data necessary for the generation of the results. The jet width is named H and is taken as a reference length scale.

3.1. Time-averaged field

Figure 2 illustrates profiles of the streamwise (z direction) components of the mean and fluctuating velocities close to jet exit (0.5H). The Figure depicts the mean streamwise velocity centerline decay as well which is an important parameter usually used to assess the accuracy and quality of numerical simulation of turbulent jets. The comparison of the previously mentioned variables with the experimental measurements of [3] are relatively acceptable. The LES simulations under-predict the fluctuating velocities close to the jet exit by up to 57%. The centerline mean velocity decay is overestimated by 5% beyond a distance of 3.2H from the jet exit. In this region, LES predicts an acceleration at 3.8H not captured by the experiments. Based on the similar profiles obtained using both the coarse and fine grids, the results obtained using the fine grid will be omitted in the subsequent section unless otherwise stated.

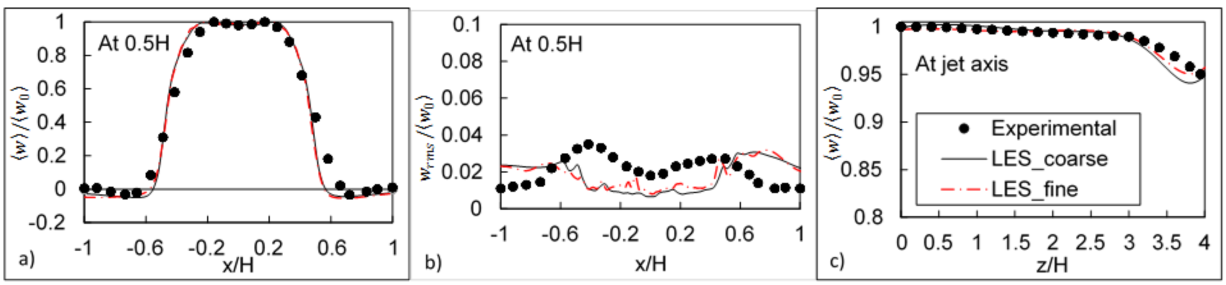

FIGURE 2. Mean and fluctuating velocity profiles at 0.5H from the inlet

3.2. Instantaneous field

Vortices are generated inside the plane shear layers surrounding the free jet region due to Kelvin-Helmholtz instabilities. They grow, sometimes in pair and in phase and interact with the slot. Figure 3 illustrates the positions of vortices having their axis in the y direction obtained from the superposition of instantaneous y vorticity contours.

The vortices follow two main trajectories upstream of the slotted impingement wall which either deviate towards the wall jet region or penetrate through the slot. The available experimental trajectories are presented by the white lines. The LES simulation complemented the picture by positions plotted within a larger domain. In the central region of the jet, upstream of the slot, vortices might access the jet core occasionally. Below the plate, the vortices generated inside the initial shear layer (close to the jet exit) and those generated at the slot lips form a plume of vortices which grows laterally by entrainment with streamwise distance. Noise generation by the intrusion of vortices into the jet core is a phenomenon that has been acknowledged previously by [20].

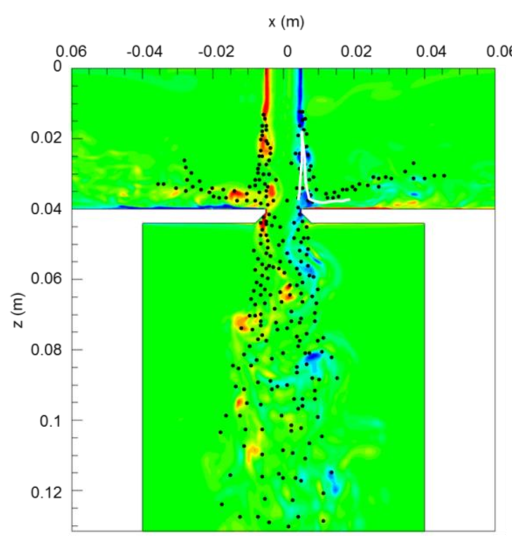

FIGURE 3. Positions of vortices (black dots) superimposed on y vorticity contours (white curves from experiments [3])

Figure 4 depicts the time-space plots of p' at four x/H positions (see Figure.1 for the positions). The time-space plots of p' show where high and low pressure regions are generated and how they are convected. The plots illustrate, also, the characteristic frequencies through the alternate low and high pressure regions with time which is approximately 213Hz. As noticed by Matsuura et al. [2], the pressure waves propagate inside the jet as well. The plots reveal roughly three zones from the jet exit towards the impingement wall (z/H<1, z/H=1-3 and z/H=3-4). The low p' regions correspond to the location of the vortices while the high p' regions correspond to the space between successive vortices. The co-rotating successive vortices entrain two opposite fluid streams which impact in the separating space causing the high pressure regions. At x/H=0, the alternate low and high pressure regions are almost vertical columns with noticeable peaks at about z/H=1.5-2.5 and close to the slot at z/H=3.5-4. These peaks correspondent to the interaction of the low and high p' regions from the opposite shear layers (see at x/H=±0.5). At x/H=±0.5, the alternate low and high p' regions are convected with a velocity equal to approximately 4.17 m/s (slop of the inclined low and high p' regions shown by dashed lines) which represents half the jet velocity. The oscillations of the jet are, also responsible for the discontinuities exhibited by the convected low and high p' regions.

At x/H=1.5, alternate perpendicular columns of p' correspond to pressure waves transmitted outside the jet region (fluid almost at rest). However, the presence of the wall jet in the zone z/H=3-4 causes the noticeable low and high p' regions such those at t=0.589s and t=0.5935s, respectively.

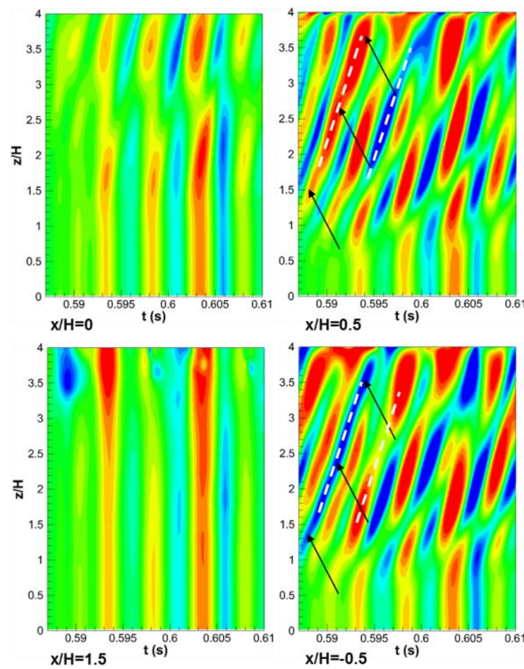

FIGURE 4. Space-time plots of pressure fluctuations at different positions x/H upstream of the impingement wall

4. CONCLUSIONS

LES was used to simulate a turbulent plane jet impinging on a slotted surface. The slot tones generated by the interaction of the jet with the slot necessitate more computational efforts compared with classical turbulent simulations. Smaller time steps, in conjunction with non-reflecting boundary conditions were used. Grid refinement gave similar results.

The centers of the vortices coincide with low pressure regions while high pressure regions reside between each two successive vortices leading to the continuous succession of low and high pressure regions from the vortex generation to their impingement on the slotted surface. Consequently, the two high pressure regions, immediately downstream of the two preceding opposite vortices, penetrate in the slot and cause the throttling phenomenon to occur which is responsible for the noticeable peaks of fluctuating pressure which in turn propagate in the rest of the domain interacting with the free-shear layer of the jet issuing from the nozzle and causing the slot tones. The pressure waves propagate, backward, inside the jet as well although their effects are not as important as those outside. The vortices follow different paths by moving into the wall jet region, penetrating into the slot or impinging on the slotted surface. The slot tones are strongly related to the behavior of the vortices which was elucidated in the present study. The acoustic field will be investigated in future work.

REFERENCES

[1] C.M. Ho, and N.S. Nosseir, Dynamics of an impinging jet. Part 1. The feedback phenomenon, *J. Fluid Mech.,* 105, 119-142, 1981.

[2] K. Matsuura, and M. Nakano, Direct computation of a hole-tone feedback system at very low Mach numbers, *J, Fluid Sci, Technol*., 6, 548-561, 2011.

[3] H. Assoum, Etude expérimentale des couplages entre la dynamique d'un jet qui heurte une plaque fendue et l'émission sonore générée, PhD Thesis, La Rochelle University, La Rochelle, France, 2013 (In French).

[4] W.K. Blake, A. Powell, The development of contemporary views of flow-tone generation, In: Recent Advances in Aeroacoustics, Springer, pp. 247-325, 1986.

[5] S. Ziada, Feedback control of globally unstable flows: impinging shear flows, *J. Fluids Struct*., 9, 907-923, 1995.

[6] M. Glesser, Sons auto-entretenus produits par l'interaction d'un jet plan avec une plaque fendue: étude expérimentale et modélisation du couplage avec un résonateur. PhD Thesis, La Rochelle University, La Rochelle, France, 2006 (In French).

[7] C.K.W. Tam, Computational Aeroacoustics: An Overview of Computational Challenges and Applications, *Int. J. Comput. Fluid Dyn*., 18, 547-567, 2004.

[8] D.J. Bodony, S.K. Lele, Current status of jet noise predictions using Large-Eddy Simulation, *A.I.A.A. J*., 46, 364-380, 2008.

[9] H. Yokoyama, M. Kobayashi, H. Onitsuka, A. Miki, A. Iida, Direct numerical simulation of flow and acoustic fields around an air-reed instrument with tone holes, Presented in 43rd International Congress on Noise Control Engineering, (inter.noise 2014), Melbourne, Australia, 2014.

[10] K. Matsuura, M. Nakano, A throttling mechanism sustaining a hole tone feedback system at very low Mach numbers, *J. Fluid Mech*., 710, 569-605, 2012.

[11] K. Matsuura, M. Nakano, Disorganization of a hole tone feedback loop by an axisymmetric obstacle on a downstream end plate, *J. Fluid Mech*., 757, 908-942, 2014.

[12] C.K.W. Tam, H. Ju, M.G. Jones, W.R. Watson, T.L. Parrott, A computational and experimental study of slit resonators, *J. Sound Vibr*., 284, 947-98, 2005.

[13] C.K.W. Tam, H. Ju, B.E. Walker, Numerical simulation of a slit resonator in a grazing flow under acoustic excitation, *J. Sound Vibr*., 313, 449-471, 2008.

[14] ANSYS Inc. Fluent User Guide and Fluent Theory Guide, 2015, version 16.2.

[15] S. Ghosal, Mathematical and physical constrains on large-eddy simulation of turbulence, *A.I.A.A. J.,* 37, 425-33, 1999.

[16] I.B. Celik, Z.N. Cehreli, I. Yavuz, Index of resolution quality for large eddy simulations, *J. Fluids Eng*., 127, 949-58, 2005.

[17] P. Sagaut, Large-eddy simulation for incompressible flows - An introduction. 3rd ed. Scientific Computation series, Berlin: Springer-Verlag; 2006.

[18] M. Hadžiabdić, K. Hanjalić, Vortical structures and heat transfer in a round impinging jet, *J. Fluid Mech.* 596, 221-60, 2008.

[19] H. Versteeg, W. Malalasekra, An introduction to computational fluid dynamics: the finite volume method. 2nd ed. Pearson Education Limited. Edinburgh Gate. Harlow. Essx CM20 2JE; 2007.

[20] C. Brehm, J. Housman, C. Kiris, Computational aeroacoustics analysis of a jet impinging on an inclined plate, A.M.S. Seminar Series at NASA Ames Research Center. https://www.nas.nasa.gov/assets/pdf/ams/2015/AMS_20150205_Brehm.pdf 33